Wafer-Scale Controlled Au/Pt Bimetallic Flowerlike Structure Array

Xing-Jiu Huang†, Ju-Hyun Kim†, Yang-Kyu Choi*

Nano-Oriented Bio-Electronic Lab, School of Electrical Engineering and Computer Science, Korea Advanced Institute of Science and Technology, Daejeon, 305-701, Republic of Korea (* e-mail:ykchoi@ee.kaist.ac.kr)
† These two authors contributed equally to this work

Abstract

The combining of the bottom-up with top-down techniques is essential to construct novel micro-/nano-materials according to the requirements of its end applications. This paper describes a pattern-directed method that combines the advantages of photolithography and electrochemical synthesis to construct a wafer-scale Au/Pt bimetallic flowerlike structure array. With this technique, Au/Pt bimetallic flowerlike structure arrays are homogeneously and highly-selectively synthesized from Au patterns with different spacing, dimensions and shapes on a 4-inch silicon wafer. The Au/Pt flowers are also well-constructed in the different designed array such as 'KAIST' and 'NOBEL'. The surface morphology of the Au/Pt flower was observed using scanning electron microscope (SEM). The chemical composition of the bimetallic flower was confirmed using energy dispersive spectrometer (EDS) and X-ray electron spectroscopy (XPS). The X-ray diffraction (XRD) patterns of the Au pitch and Si substrate on a wafer were studied to reveal the highly-selective growth from Au pitches. A time-dependent evolution clearly presents the different growth stages of Au/Pt flower. The analysis of Au/Pt flower growth process in an individual Au pitch shows an edge-selective particle development mechanism. The method can be applied to the construction of other interesting nano/microflower arrays of metals or metal oxides. The results would be helpful for the creation of the flower with regular physical attributes (shapes and sizes) and guiding the design of a perfect array for technological innovations.

Introduction

Photolithography is the most widely and currently used technique among several standard lithographic methods to create nano/microstructures (1-3). The most important advantage is that the size, shape, and interparticle spacing of such a structure is determined by the requirements of its end application rather than the chemical and physical forces that direct its formation (4-6). Bimetallic nanoparticles are considered to be a mainstay of commercial heterogeneous catalysts and are employed in a variety of industrial catalytic reactions (7). Bimetallic Au/Pt nanoparticles are of fundamental interest and importance due to their optical properties (8) and range of potential catalytic activities (9-12). Therefore, their synthesis and characterization have been attracting active attention (7,13-23). Especially, Eychmüller reported ordered Au/Pt bimetallic nanostructures based on hollow silica spheres (22). Yang reported electrochemical fabrication of Au-Pt bimetallic flowerlike nanostructures on a polyamidoamine dendrimers modified indium tin oxide surface (23). However, no flowerlike structures with regular physical attributes (shapes and sizes) or arrays have been addressed thus far. In a number of earlier reports regarding nanoparticles array, colloidal sphere array templates were typically used for fabricating the structure (22). However, these methods are often limited in terms of homogeneity and have uncontrollable array shapes. In addition, Raj *et al.* and Shi *et al.* have suggested that the surface morphology and the shape of metal particles, such as flowerlike morphology (24,25), play an important role in obtaining a high electrocatalytic activity. However, the random aligning of the particles in these studies restricts a development for the controllability of nanodevices or nanosensors in the potential applications.

For longer term applications, therefore, it is of great significant to develop an alternative and controllable method to directly produce well-defined Au/Pt flowerlike structure array to meet the requirements for potential application in several fields such as nanodevices and nanosensors, etc. In this study, we present a pattern-directed method that combines the advantages of photolithography and electrochemical synthesis to construct a wafer-scale Au/Pt bimetallic flowerlike structure array. With this technique, Au/Pt bimetallic flowerlike structure arrays are homogeneously and highly-selectively synthesized from Au patterns on a 4-inch silicon wafer. The shape and position of the arrays and the position and the density of the Au/Pt flower in the array are well-controlled according to the end requirements.

Experimental

Fabrication of Au Pattern

The Au pattern was prepared using a photolithography technique. The starting substrate was a 4-inch p-type silicon wafer with a thickness of 525 μm. First, the silicon wafer was

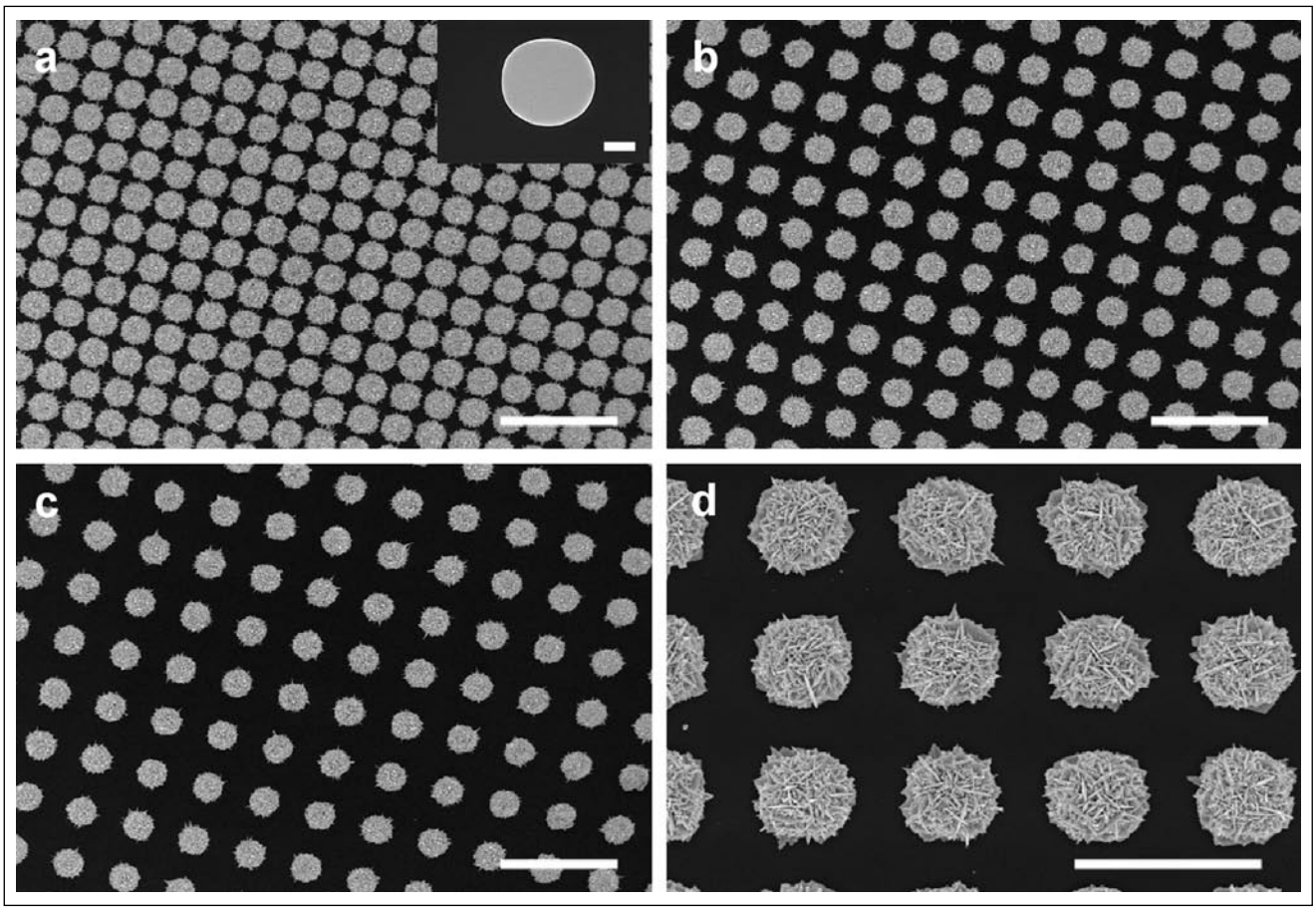

Figure 1

SEM images of an Au/Pt bimetallic flower array taken on spacing of the 4 μm (a), 6 μm (b) and 8 μm (c) Au patterns after deposition. The scale bar is 20 μm (2500×). A symmetric circular Au pattern with dimension of 2 μm (shown in the inset of panel a, scale bar is 2 μm) was utilized. d, A typical high-magnification SEM image of the prepared flower array. The scale bar is 10 μm (8000×). The experiments were performed at $PtCl_6^{2-}/AuCl_4^-$ mole ratio of 2:5, an applied potential of 0.3 V and deposition time of 60 min unless specially designated

cleaned using a 1:100 diluted HF solution for 30 sec to remove the native oxide layer, 10 nm of a Cr layer and 100 nm of an Au layer were then sequentially deposited onto the silicon wafer by thermal evaporation. The deposited Cr layer acted as a glue layer between the silicon substrate and the Au layer. Second, a photoresist pattern was defined by optical photolithography using G-line ultraviolet light with a wavelength of 436 nm and an AZ6612KE positive photoresist. The photoresist patterns were used as a hard mask for a subsequent Au/Cr wet etching process. In order to transfer the photoresist patterns to the Au layer, a 1:100 diluted KCN solution was used as a wet etchant for the Au layer. The wet etching process was performed at 25°C for 60 sec. After the etching process of the Au layer, the remaining Cr layer was etched using a CR-7 Cr etchant at 25°C for 30 sec. Finally, all photoresist patterns were removed using acetone and AZ400T, a photoresist remover, at 50°C for 1 hour. The Au patterned silicon wafer was then rinsed using deionized water (DIW) and was blow dried.

Formation of Au/Pt Bimetallic Flower Array

The Au/Pt bimetallic flower array was synthesized in an aqueous solution containing H_2PtCl_6 ($H_2PtCl_6{\cdot}6H_2O$, Sigma Aldrich), $HAuCl_4$ ($HAuCl_4{\cdot}3H_2O$, Sigma Aldrich), and 20 g l^{-1} polyvinylpyrrolidone (K30, Fluka) using a two-electrode system. The cleaned Au pattern was employed as a working electrode and a clean graphite sheet served as counter electrode. The applied potential was controlled using a Triple Output DC power supply (Agilent, E3631A).

Materials Characterization

Sample morphologies were investigated using Philips XL 30 AFEG scanning electron microscope (SEM, Eindhoven, The Netherlands). Energy dispersive spectrometer analysis (EDS) was carried out using an EDAX system (Phoenix, EDAX International Corporation). X-ray electron spectroscopy (XPS) was performed using a VG ESCA 2000 X-ray photoelectron spectrometer with an $Mg_{k\alpha}$ excitation source. X-ray diffraction (XRD) pattern were measured on a diffractometer (Philips XGpert PRO with $Cu_{k\alpha}$ radiation).

Results and discussion

The Au patterns were initially fabricated using photolithography, and Au/Pt bimetallic flowers were then directedly electrosynthesized onto an Au pattern. SEM images were collected to demonstrate the results of experiments

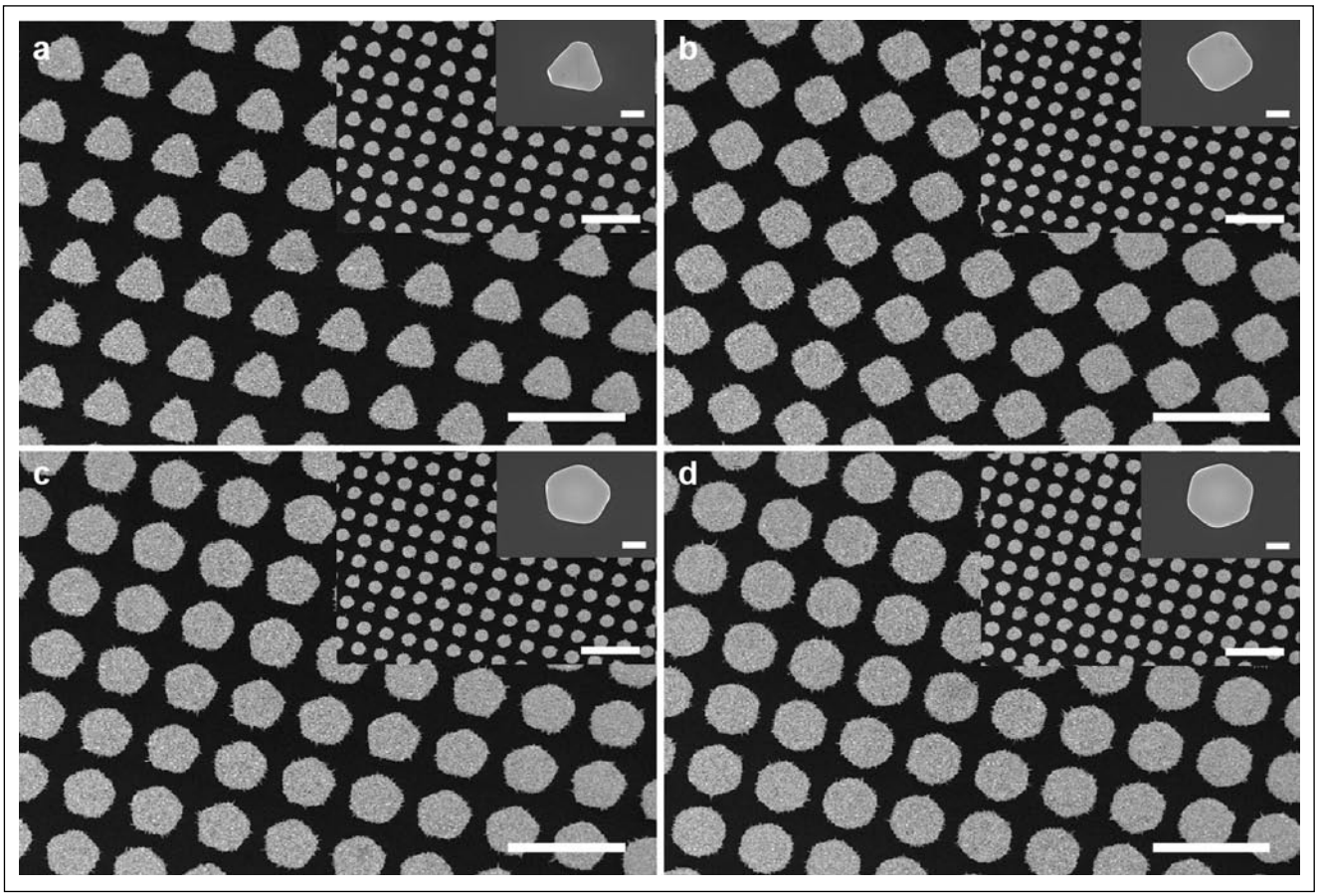

Figure 2

SEM images of an Au/Pt bimetallic flower array grown from an Au pattern with different dimensions and shapes. a-d, Images taken on triangular (a), rectangular (b), pentagonal (c) and hexagonal (d) patterns with the dimension of 6 μm. The scale bar is 20 μm (2500×). The insets in a, b, c and d show the Au/Pt bimetallic flower array on the corresponding pattern with a dimension of 2 μm, respectively. The scale bar is 20 μm (2500×). The small SEM images located at the upper right corner in each image show the corresponding individual bare Au patterns. The scale bar is 2 μm (20000×)

described above. Figures 1a, b and c show the evolution of the Au/Pt particles array synthesized onto 2 μm of Au patches array surface with different spacing of the 4 μm (Figure 1a), 6 μm (Figure 1b) and 8 μm (Figure 1c). As depicted in these low-magnification SEM images, the Au/Pt particles were determined to be highly-selectively synthesized from all the Au patches simultaneously. Nothing was found on the silicon substrate. This case can also be clearly distinguished using a high-magnification scanning electron microscope image shown in Figure 1d. Interestingly, from this closer examination, we observed that each Au/Pt particle in the array presents a natural flowerlike structure, and a single flower carries many leaves (i.e., many nanoscaled flakelike blocks). The overall process approximately requires 60 min to get such a developed flowerlike structure. We should emphasize that the dimension of 2 μm of Au patch used in the example ensures the formation of Au/Pt flower. In fact, the dimension of an Au patch has a significant effect on the bimetallic flower, as will be considered in more detail in the following section.

Figure 2 shows the evolution of an Au/Pt bimetallic array deposited on an Au pattern with different dimensions and shapes (triangular, rectangular, pentagonal and hexagonal). The SEM image reveals that the Au/Pt bimetallic particles can be highly selectively deposited on the Au pattern (~ 6 μm) in different shapes; it also shows that a regular array with few defects can form. However, an Au/Pt flowerlike structure was not produced, although a number of leaflike flakes were observed on the pattern surface. It is suggested that in this study, the lateral-directional growth rate may be faster than the vertical rate for a larger Au pitch. Besides, as investigated a high-magnification SEM image of bimetallic Au/Pt on a single rectangular patch (~ 6 μm, data not shown here), it shows a truncated rectangular pyramid structure. The four sides slowly shrink to form a pyramidal structure and then a flowerlike structure if underwent a long period of deposition. In contrast, an Au/Pt flower array easily forms on a pattern with a dimension of ~ 2 μm (The insets of Figure 2). This result suggests that the formation of the Au/Pt bimetallic flowerlike structure cannot be attributed to the shape but to the dimension of the Au patch.

To further demonstrate the controllability of this pattern-directed method to construct flower array, we studied the growth of Au/Pt bimetallic flower on the surfaces of different engineered patterns. Figure 3a is a low-magnification SEM image of a designed 'KAIST' and 'NOBEL' word pattern after deposition, which shows a large area of the highly-selective growth of the Au/Pt bimetallic structure. A closer examination

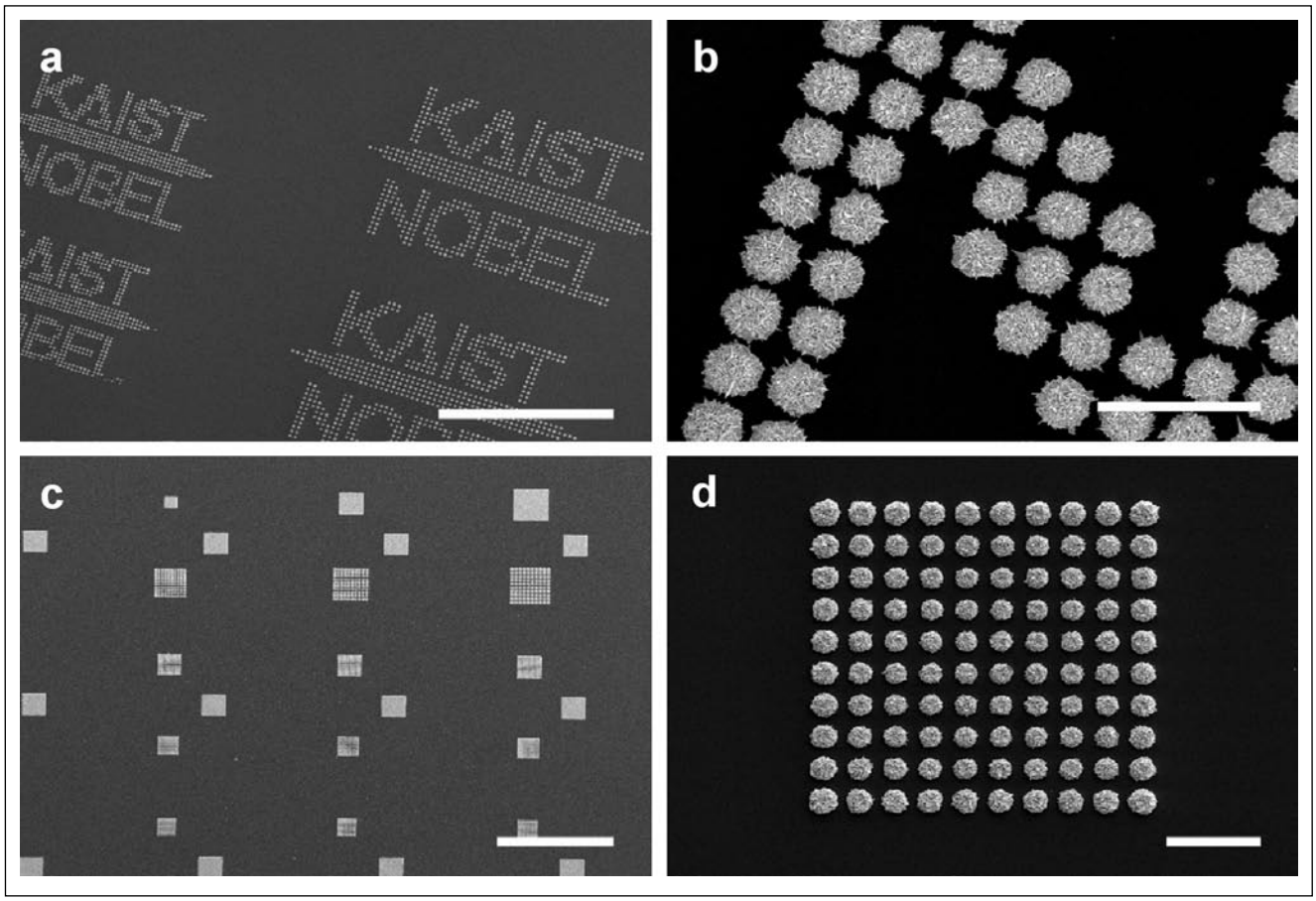

Figure 3

SEM images of an Au/Pt bimetallic flower taken on different designed array. (a) The final state of the 'KAIST' and 'NOBEL' pattern (abbreviation of the related university and laboratory names) where the Au/Pt bimetallic flower covers the whole of each Au pattern. The scale bar is 500 μm (150×). (b) A high-magnification SEM image of the letter "N". The scale bar is 20 μm (3500×). (c) A low-magnification SEM image of a large-scale designed array after electrodeposition. The scale bar is 500 μm (100×). (d) A 10×10 Au/Pt bimetallic flowerlike structure array grown on an Au circular pattern with a dimension of 1 μm. The scale bar is 20 μm (2000×)

shown in Figure 3b clearly demonstrates a flowerlike structure array. A representative Au pattern was also designed with a quadrangular and linear shape for Au/Pt bimetallic flower deposition (Figure 3c). In a 10×10 array (Figure 3d), the well-defined Au/Pt bimetallic flowers array does not appear to be more 'homogeneous' or 'uniform', as the outside flowers are typically bigger than inside ones. This case can be ascribed to a flower growth mechanism for the entire pattern. In fact, the variation of the size has good regularity. To explain the flower position clearly, this array was divided into different layers from outside to inside. The four flowers respectively located in the four corners have the largest size and then gradually decreases in three different directions. The four flowers in the central part of this array have the smallest size. Additionally, the center point of four sides in each layer represents the smallest structure, and the corresponding size gradually decreases from the outermost to the innermost layer.

The chemical composition of the Au/Pt bimetallic flower was determined using an energy dispersive spectrometer analysis, as shown in Figure 4a. In the EDS spectrum, the strong peaks of PtMa, AuMa, PtLa, and AuLa come from bimetallic flower, the Si peak originates most likely from the silicon wafer, and the appearance of the very weak peaks of C, N, and O can be attributed to polyvinylpyrrolidone on the 'petal' surface, which is used to prevent the Au/Pt bimetallic particles from agglomerating. This proposal is further supported by an X-ray electron spectroscopy experiment (Figure 4b). As noted from the wide-scan spectrum, key information concerning the chemical state of the prepared flower is known. Firstly, O 1s signal is observed at 534.02 eV which is no obvious shifts between Au monometallic and Au/Pt bimetallic particles, indicating that the C=O group is not affected by the bimetallic flowers. Secondly, N 1s peak at 400.0 eV is usually observed for Au monometallic particles (15), but it shifts to 401.0 eV here which maybe due to the positive charged nitrogen atoms after attached Au/Pt bemetallic flowers. More direct evidences are from the high-resolution Au $4f_{5/2}$, Au $4f_{7/2}$, Pt $4f_{5/2}$, and Pt $4f_{7/2}$ spectra shown in the insets in Figure 4b. The Au 4f doublet is identified at 88.0 and 84.0 eV for Au $4f_{5/2}$ and Au $4f_{7/2}$, respectively. The Pt XPS spectrum is deconvoluted into two pairs of doublets with peaks centered at binding energies of 71.0 and 74.9 eV, respectively. These two peaks are attributed to Pt $4f_{7/2}$ and Pt $4f_{5/2}$ excitations of metallic platinum. On the basis of the above SEM, EDS, and XPS analyses, it is realistic to conclude that Au/Pt bimetallic flowerlike structure arrays were formed.

To understand how the Au/Pt flower arrays were controllably formed, the nucleation mechanism of Au/Pt flowerlike particles was studied. It has been demonstrated that, during the electrodeposition process, the nucleation mechanism of metal on a substrate is strongly dependent upon the surface orientation and the deposition potential (26). Therefore, the XRD patterns of the Au pitch and Si substrate on a wafer were studied (Figures 5a and b). The intensity ratio of the {200} and {111} diffraction peaks in the XRD pattern of the Au pitch was 0.15, which is lower than the bulk value of 0.53, suggesting that the Au pitch structures on the wafer were abundant in the {111} planes and, thus that {111} planes tended to be preferentially oriented parallel to the surface of the Si wafer. This suggests that the nucleation of Au/Pt flowerlike particles on {111} Au easily occurs at V_{appl} = 0.3 V, rather than on the {311} Si planes (Figure 5b). Further confirmation regarding the significant effect of the deposition potential is found by depositing Au particles on Au pitches (Figures 5c and d). Au particles were observed to cover the entire wafer at V_{appl} = 1.5 V. From these experiments, it was concluded that the controllability of Au/Pt flower electrodeposition can be attributed to the nucleation mechanism.

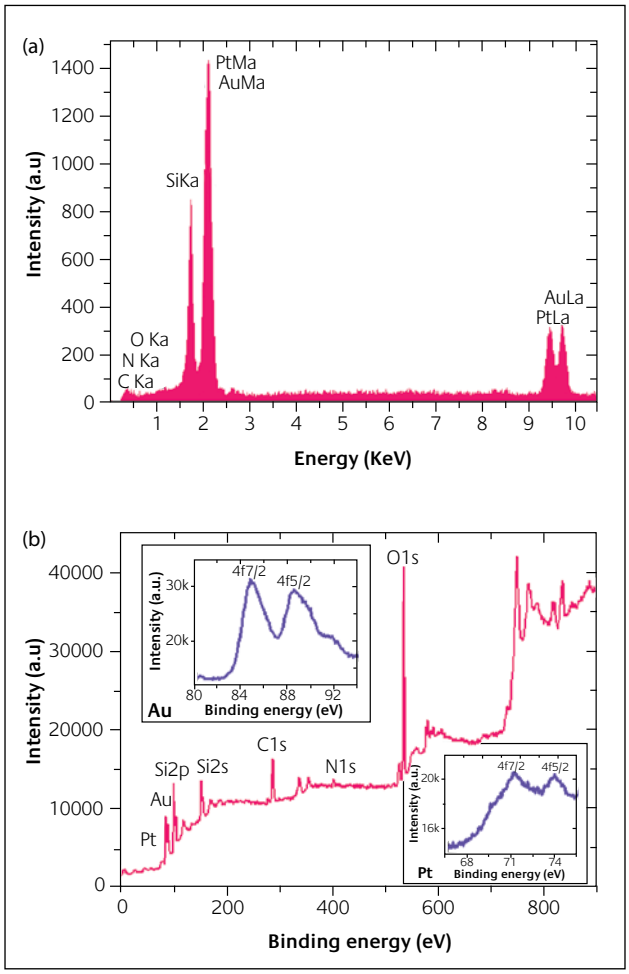

Figure 4

EDS analysis (a) and XPS analysis (b) of the Au/Pt flowerlike structure array shown in this study. The insets in panel b show the high-resolution Au4f$_{5/2}$, Au4f$_{7/2}$, Pt4f$_{5/2}$, and Pt4f$_{7/2}$ spectra

The time-dependent evolution of a highly selective Au/Pt bimetallic flower on an Au square pattern was recorded by SEM images (Figure 6) to understand the growth process. Clearly, very few Au/Pt bimetallic particles grew on the Au patch sparsely and randomly within a few seconds (Figure 6a). During the following deposition period from 5 min to 10 min, a number of Au/Pt bimetallic leaflike flakes appear on the square surface, and the shape changes from a square (Figure 6b) to a circle (Figure 6c), gradually resulting in a simple flowerlike structure. Surprisingly, an 'ugly' hump formed due to the many small clusters and needlelike particles, as observed after 20 min (Figure 6d). This case can be considered as the process of Au/Pt nucleation which is in agreement with previous reports on electrosynthesis of metal particles (25). However, a fine flowerlike structure can be seen clearly again after continuous deposition (Figure 6e). At this stage, the shape is similar to a previous one (Figure 6c), and the structure becomes more complicated. Hence, the 'ugly' hump is likely a very important intermediate structure. Upon increasing the deposition time further, the flowerlike structure continues to grow and eventually expands into a fully developed complex flowerlike architecture ~ 6 µm in diameter (Figure 6f) as expected. It was observed that the physical attributes of the Au/Pt flower are fairly different from those in a previous report (23), which includes many leaflike flakes with sharp edges and corrugated surface. Some leaflike flakes are interdigitatedly arranged around the flower and form a multilayer structure, which emanates from the cores to the outside. Numerous gaps between the interdigitated flakes can be observed. Interestingly, in the central part, the flakes are nearly arranged in a perpendicular direction to the outside flakes, as in the 'pistil/stamen' arrangement of a flower. It has been demonstrated that the presence of sharp edges or tips in metal nanoparticles increases the electric-field enhancement, which is important for applications as sensors (27). Additionally, the morphologies of Au/Pt bimetallic nanoparticles can affect their catalytic activities, which are different from those of individual nanoparticles (7,13). It is therefore believed that the Au/Pt bimetallic flower structure array involving in many self-governed flowers may be particularly suitable for catalytic applications, although future studies will be required to demonstrate this contribution. By analyzing the dimension of leaflike flakes in time-dependent evolution, it is concluded that the growth of Au/Pt flakes follows progressive nucleation where new nuclei are gradually formed in time (26,28,29), and in which a wide distribution of nuclei with different dimensions can be expected. Considering the theory of low surface free energy, the individual leaflike flakes readily symmetrically assemble to form a flowerlike structure in a rotary type due to electrostatic interactions according to the arrangement order of a natural flower petal.

The growth of flower generally needs receptacles that are commonly observed in nature. Developing the mechanism of synthetic formation of such microflower oriented nanostructures on Au patch remains a significant challenge.

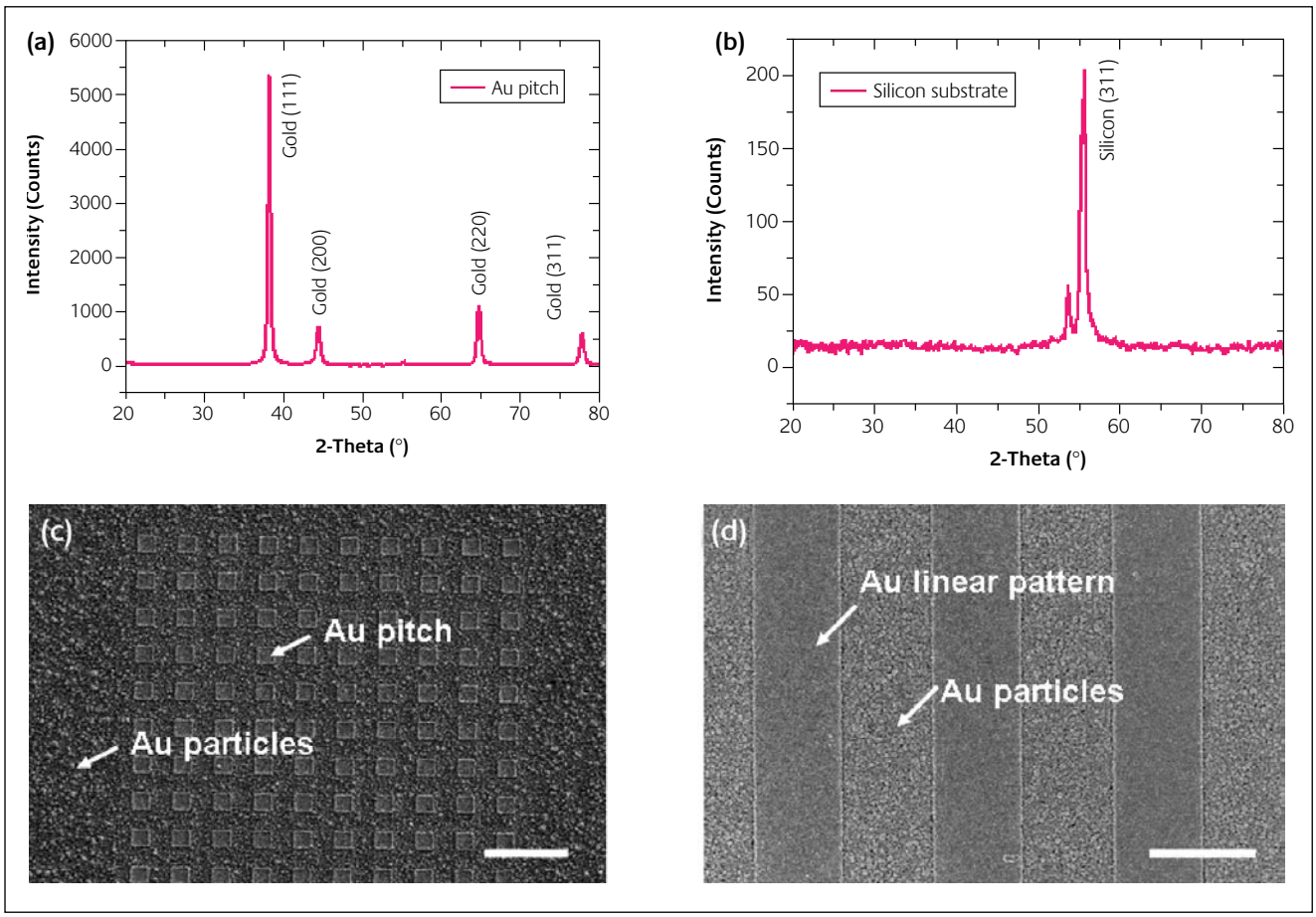

Figure 5

XRD patterns of the Au pitch (a) and silicon substrate (b) for the Au/Pt flower array deposition. SEM images of the patterned Au particles deposition at a potential of 1.5 V (c, d). The scale bars in c and d are 20 and 10 µm, respectively

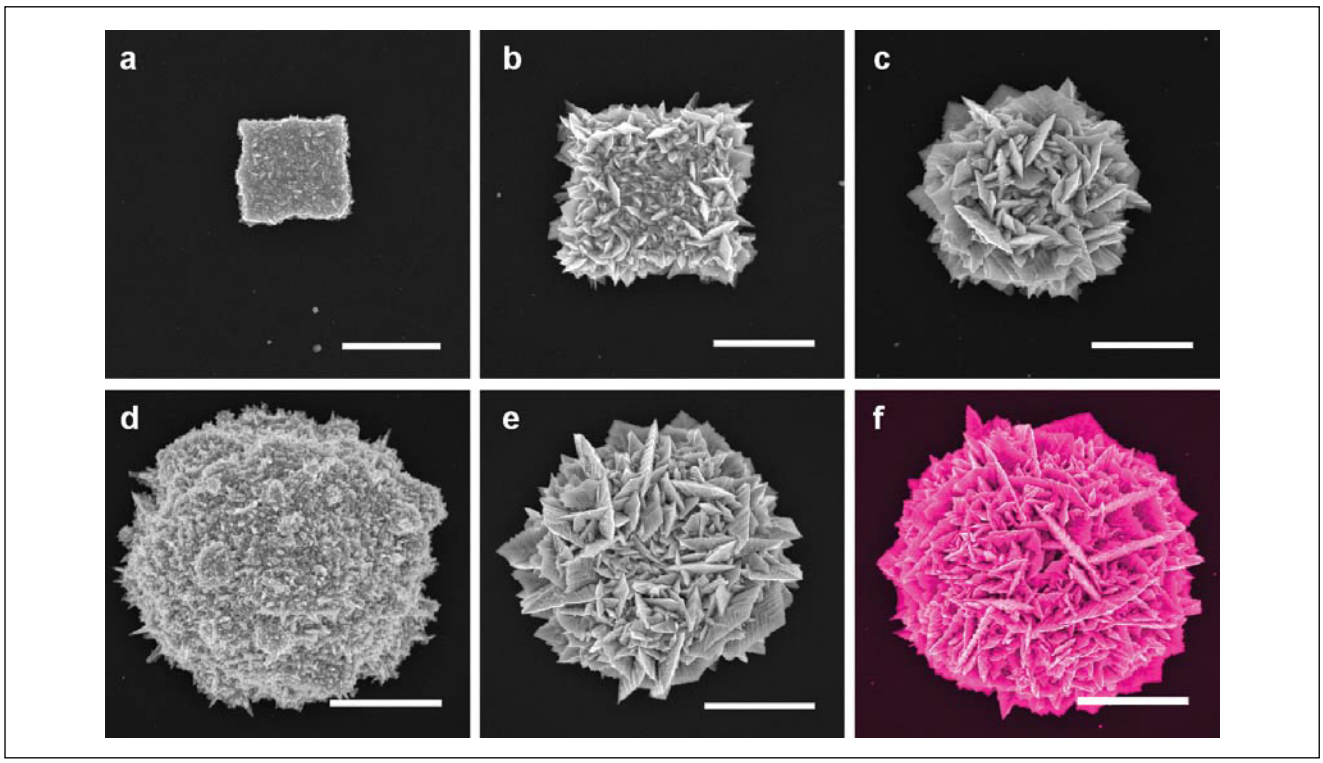

Figure 6

*Time-dependent evolution of an Au/Pt bimetallic flowerlike structure grown from a rectangular pattern at different growth stages. a-f, Images taken 10 sec (**a**), 5 min (b), 10 min (c), 20 min (d), 30 min (e), and 90 min (f) after deposition. The scale bars in a, b and c are 1 µm, and those in d, e and f are 2 µm, respectively*

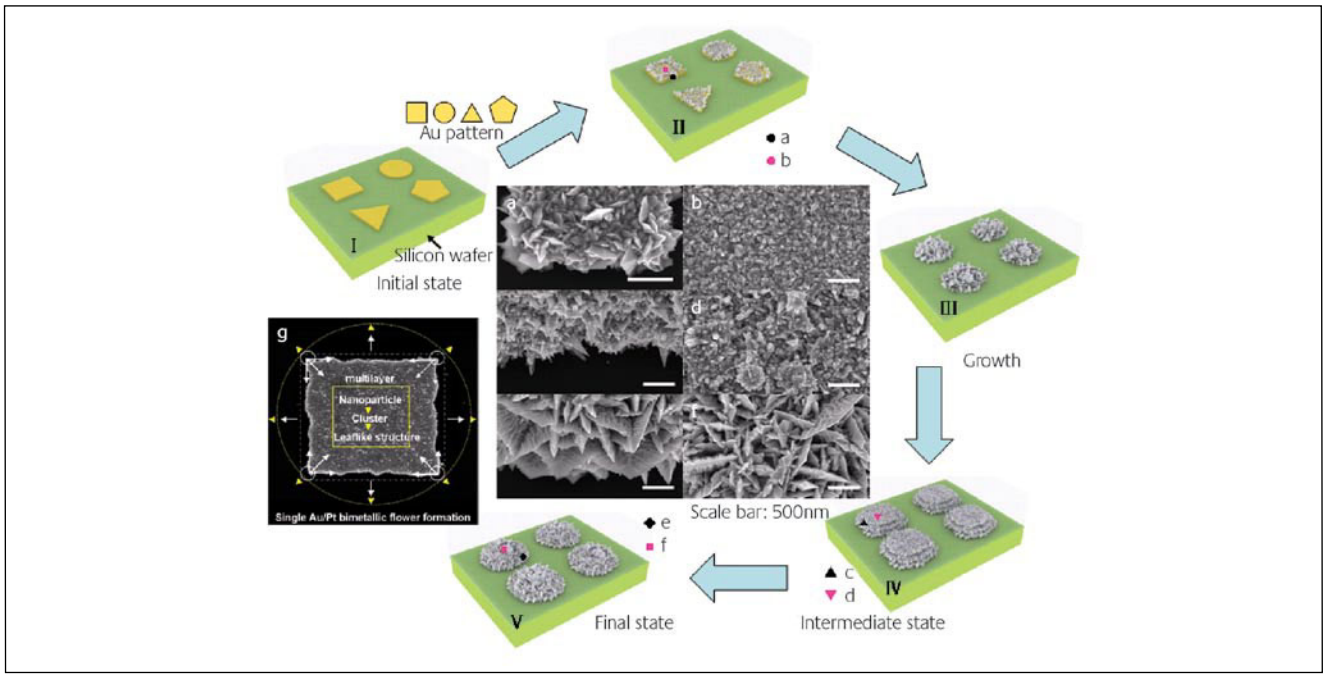

Figure 7

Sketch of the experimental set-up for Au/Pt bimetallic flower array structuring. I-V, Sketch of the Au/Pt bimetallic flower array structuring. a-f, SEM images taken in support of a number of important processes described in the sketch. I, Au patterns with different shapes were fabricated on a silicon wafer using a photolithography technique and employed as a cathode in a $PtCl_6^{2-}/AuCl_4^-$ solution. II, After electrodeposition for several minutes, several leaflike flakes of Au/Pt particles (a) were observed at the edge of the pattern and several other shape particles (b) were observed in the central part of the Au patches. The growth of the Au/Pt was confined to the Au patches. III, Au/Pt particles with a simple flower structure are formed. IV, A transient state of the Au/Pt flower formation is shown at 20 min. Needle-like particles (c) at the edge and many clusters (d) in the central part of the structure can be observed. V, The final morphology with the full flower structure on each Au pattern is shown at 90 min. From the corresponding SEM images, different arrangement format of the leaflike flakes were observed at the edge (e) and in the central part (f) of the Au/Pt flower. g, Schematic illustrations for the shape progression of a single Au/Pt bimetallic flower on an Au square

Based on the experimental observations above, however, it is suggested that the observed Au/Pt flower array growth process in an individual Au pitch occurs through an edge-selective particle development mechanism involving four steps (Figure 7). The role of the Au patches (Figure 7I) is just like receptacles. The Au/Pt bimetallic flower grows from the edge to the central part, and the pattern shape is still observed at this stage (Figure 7II). In the early stages of growth, Au/Pt particles sparsely grow along the Au patches orientation, the {111} direction. These particles consist mostly of undefined structures with a wide size distribution. However, as the randomly oriented particles grew further, they began to overlap and their growth became physically limited as the misaligned particles began to impinge on other neighbouring particles, resulting in a compact film (figure 7b). But we can observe some flakelike particles at the edge of the patch (figure 7a). In this stage, taking a rectangle patch as an example, Au/Pt bimetallic particles grow from four corners to central part (Figure 7h). Consequently, the particles grow from the four edges of the patch to outside (radial growth process). Because of a similar rate of radial and flowerlike growth on the substrate, a simple flower structure with a circular shape is gradually formed (Figure 7III). Through an intermediate structure of nucleation (Figure 7IV, Figures 7c and d clearly shows the morphology of the edge and central part of this stage, respectively), a fully developed flower is obtained (Figure 7V, nanoflakes were produced in the edge and central part, as shown in Figures 7e and f). The overall process of the formation of an individual flower, for example a square pattern, is illustrated in Figure 7g. Finally, an investigation of the $AuCl_4^-/PtCl_6^{2-}$ mole ratio effect on the formation of Au/Pt bimetallic flower at constant applied potential and deposition time was conducted, and we discovered a stoichiometry-dependent process, which results in the formation of flowerlike or undefined structure with different surface features, under one set of conditions. So the mole ratio of $AuCl_4^-/PtCl_6^{2-}$ plays a key role in the flower formation.

Conclusions

A pattern-directed technique that can be used for the synthesis of controllable arrayed Au/Pt flower particles with regular physical attributes is thus demonstrated. The detailed experiments and analyses indicate that it opens a door for exploring a topical area of photolithography technique and materials science. SEM images reveal the Au/Pt flower has regular physical attributes (shapes and sizes) and the arrays are highly-selectively synthesized from Au patches. The formation of the Au/Pt bimetallic flowerlike structure cannot be attributed to the shape (triangular, rectangular, pentagonal and hexagonal)

but to the dimension (~ 2 μm) of the Au patch in a given deposition time. The flowerlike structure will benefit from smaller patches. The controllability of Au/Pt flower array on a silicon wafer can be attributed to the nucleation of Au/Pt flowerlike particles on {111} Au easily occurs at V_{appl} = 0.3 V, rather than on the {311} Si planes. This suggestion can be supported by the deposition on a designed 'KAIST' and 'NOBEL' pattern. Therefore, the presented method can be applied to the construction of other interesting nano/microflower arrays of metals or metal oxides using specially predesigned structural pattern with a nucleation nature and optimized potential. Although the formation mechanism of flowerlike structure has not been fully understood yet, this technique would offer us an opportunity for the creation of the highly controllable synthesis of flower arrays with extremely high surface-to-volume ratio, and may enable flowerlike structure-based devices such as DNA chips and high-density or density-/position-controlled sensor arrays to be produced. Research along these lines would result in wide applications for this new technique and is currently underway.

About the authors

Dr. Xing-Jiu Huang is a research professor in the School of Electrical Engineering and Computer Science at Korea Advanced Institute of Science and Technology (KAIST). His research focuses on the synthesis of nanomaterials, bio-electronic sensors, chemical sensors, and novel nanomaterial assemblies.

Ju-Hyun Kim is a Ph.D candidate in the School of Electrical Engineering and Computer Science at KAIST. His research under the direction of Prof. Choi focuses on the bio-electronic sensors and novel device fabrication.

Dr. Yang-Kyu Choi is an associate professor in the School of Electrical Engineering and Computer Science at KAIST. His research interests include multiple-gate MOSFETs, exploratory devices, and novel memory devices, nanofabrication technologies for bioelectronics, as well as nanobiosensors.

Acknowledgements

Dr X. J. Huang would like to express appreciation for the financial support of the Brain Korea 21 project, the School of Information Technology, Korea Advanced Institute of Science and Technology in 2007. It was partially supported by the National Research and Development Program (NRDP, 2005-01274) for biomedical function monitoring biosensor development sponsored by the Korea Ministry of Science and Technology (MOST), and partially supported by NRL program of the Korea Science and Engineering Foundation grant funded by the Korea government (MOST) (NO. RøA-2007-000-20028-0).

References

1 J. Léopoldès, P. Damman, *Nature Mater.*, 2006, **5**, 957
2 C. L. Haynes, R. P. Van Duyne, *J. Phys. Chem. B*, 2001, **105**, 5599
3 N. Feth, C. Enkrich, M. Wegener, S. Linden, *Opt. Express*, 2007, **15**, 501
4 G. M. Wallraff, W. D. Hinsberg, *Chem. Rev.*, 1999, **99**, 1801
5 T. Ito, S. Okazaki, *Nature*, 2000, **406**, 1027
6 D. Dendukuri, D. C. Pregibon, J. Collins, T. A. Hatton, P. S. Doyle, *Nature Mater.*, 2006, **5**, 365
7 H. F. Lang, S. Maldonado, K. J. Stevenson, B. D. Chandler, *J. Am. Chem. Soc.*, 2004, **126**, 12949
8 T. Shiraishi, K. Hisatsune, Y. Tanaka, E. Miura, Y. Takuma, *Gold Bull.*, 2001, **34**, 129
9 C. Mihut, C. Descorme, D. Duprez, M. D. Amiridis, *J.Catal.*, 2003, **212**, 125
10 J. Shen, J. M. Hill, M. W. Ramachandra, S. G. Podkolzin, J. A. Dumesic, *Catal. Lett.*, 1999, **60**, 1
11 Y. Lou, M. M. Maye, L. Han, J. Luo, C. J. Zhong, *Chem. Commun.*, 2001, **5**, 473
12 D. C. Skelton, H. Wang, R. G. Tobin, D. K. Lambert, C. L. Dimaggio, G. B. Fisher, *J. Phys. Chem. B*, 2001, **105**, 204
13 S. H. Zhou, K. McIlwrath, G. Jackson, B. Eichhorn, *J. Am. Chem. Soc.*, 2006, **128**, 1780
14 D. I. Garcia-Gutierrez, C. E. Gutierrez-Wing, L. Giovanetti, J. M. Ramallo-López, F. G. Requejo, M. Jose-Yacaman, *J. Phys. Chem. B*, 2005, **109**, 3813
15 C. W. Chen, T. Serizawa, M. Akashi, *Chem. Mater.*, 2002, **14**, 2232
16 H. M. Chen, H. C. Peng, R. S. Liu, S. F. Hu, L. Y. Jang, *Chem. Phys. Lett.*, 2006, **420**, 484
17 A. Henglein, *J. Phys. Chem. B*, 2000, **104**, 2201
18 B. Zhang, J. F. Li, Q. L. Zhong, B. Ren, Z. Q. Tian, S. Z. Zou, *Langmuir*, 2005, **21**, 7449
19 R. M. Crooks, M. Q. Zhao, L. Sun, V. Chechik, L. K. Yeung, *Accounts Chem. Res.*, 2001, **34**, 181
20 N. Dimitratos, L. Prati, *Gold Bull.*, 2005, **38**, 73
21 D. C. Skelton, H. Wang, R. G. Tobin, D. K. Lambert, C. L. DiMaggio, G. B. Fisher, *J. Phys. Chem. B*, 2001, **105**, 204
22 L. H. Lu, R. Capek, A. Kornowski, N. Gaponik, A. Eychmüller, *Angew. Chem. Int. Ed.*, 2005, **44**, 5997
23 L. Qian, X. R. Yang, *J. Phys. Chem. B*, 2006, **110**, 16672
24 B. K. Jena, C. R. Raj, *Langmuir* 2007, **23**, 4064
25 Y. Li, G. Q. Shi, *J. Phys. Chem. B* 2005, **109**, 23787
26 L. M. Depestel, K. Strubbe, *J. Electroanal. Chem.*, 2004, **572**, 195
27 K. L. Kelly, E. Coronado, L. L. Zhao, G. C. Schatz, *J. Phys. Chem. B*, 2003, **107**, 668
28 B. R. Scharifker, J. Mostany, *J. Electroanal. Chem.*, 1984, **177**, 13
29 G. Gunawardena, G. Hills, I. Montenegro, B. Scharifker, *J. Electroanal. Chem.*, 1982, **138**, 225